

# *Spitzer*/MIPS Limits on Asteroidal Dust in the Pulsar Planetary System PSR B1257+12

G. Bryden<sup>1</sup>, C. A. Beichman<sup>2</sup>, G. H. Rieke<sup>3</sup>,  
J. A. Stansberry<sup>3</sup>, K. R. Stapelfeldt<sup>1</sup>, D. E. Trilling<sup>3</sup>, N. J. Turner<sup>1</sup>, & A. Wolszczan<sup>4</sup>

1) *Jet Propulsion Lab, 4800 Oak Grove Dr, Pasadena, CA 91109*

2) *Michelson Science Center, California Institute of Technology, Pasadena, CA 91125*

3) *Steward Observatory, University of Arizona, 933 North Cherry Ave, Tucson, AZ 85721*

4) *Department of Astronomy and Astrophysics, Pennsylvania State University, University  
Park, PA 16802*

bryden@jpl.nasa.gov

## ABSTRACT

With the MIPS camera on *Spitzer*, we have searched for far-infrared emission from dust in the planetary system orbiting pulsar PSR B1257+12. With accuracies of 0.05 mJy at 24  $\mu\text{m}$  and 1.5 mJy at 70  $\mu\text{m}$ , photometric measurements find no evidence for emission at these wavelengths. These observations place new upper limits on the luminosity of dust with temperatures between 20 and 1000 K. They are particularly sensitive to dust temperatures of 100-200 K, for which they limit the dust luminosity to below  $3 \times 10^{-5}$  of the pulsar's spin-down luminosity, three orders of magnitude better than previous limits. Despite these improved constraints on dust emission, an asteroid belt similar to the Solar System's cannot be ruled out.

*Subject headings:* infrared: stars — circumstellar matter — pulsars:individual(PSR B1257+12)

## 1. Introduction

Before the discovery of extrasolar planets around main-sequence stars (Mayor & Queloz 1995; Marcy & Butler 1995), pulsar timing measurements provided the first evidence for an extrasolar planetary system (Wolszczan & Frail 1992). The initial discovery of two planets was later expanded to three:  $0.02 \pm 0.002 M_{\oplus}$  at 0.19 AU,  $4.3 \pm 0.2 M_{\oplus}$  at 0.36 AU, and

$3.9 \pm 0.2 M_{\oplus}$  at 0.46 AU (Wolszczan 1994; Wolszczan et al. 2000; Konacki & Wolszczan 2003). Orbital analysis of the pulsar timing measurements reveals a coplanar system with the outer planets in 3:2 orbital resonance (Konacki & Wolszczan 2003), strongly suggesting that their formation mechanism must involve a preplanetary disk of material circling the neutron star. A variety of theories have been proposed for the formation of such a disk in this system (see Miller & Hamilton 2001) - from the remains of a merger event (Podsiadlowski et al. 1991), from the disruption or ablation of a stellar companion (Stevens et al. 1992; Tavani & Brookshaw 1992), or from the fall back of supernova ejecta (Lin et al. 1991). The presence of an early disk is further motivated by theories for millisecond pulsar formation, which generally use an accretion disk to spin up the pulsar (Michel & Dessler 1985).

In its presumed disk origin, the pulsar system’s history is thought to be similar to our own Solar System and its protostellar nebula. Evidence for such disks around hydrogen-burning stars is clear. Massive protoplanetary disks are commonly found in young star forming regions, both inferred from spectral energy distributions (Beckwith et al. 1990) and seen directly in silhouette (McCaughrean & O’Dell 1996). The older remnants of these disks were first discovered around main sequence stars by IRAS (Aumann et al. 1984), with many debris disks later identified by ISO (Habing et al. 2001) and now with *Spitzer* (Rieke et al. 2005). Dusty disks are frequently found around main sequence stars over a range of spectral types and ages, yet no disk emission has ever been detected from around a pulsar.

Many attempts have been made to survey nearby pulsars for dust emission. The broadest of these surveys, an examination of the positions of 478 pulsars in the IRAS Point Source Catalog, failed to identify any excess beyond that expected from coincidental alignment (van Buren & Terebey 1993). Many smaller but more sensitive surveys of pulsars have been made, both in the infrared (Foster & Fischer 1996; Koch-Miramond et al. 2002; Lazio & Fischer 2004) and at sub-mm wavelengths (Phillips & Chandler 1994; Greaves & Holland 2000; Löhmer et al. 2004). As the host to a planetary system, PSR B1257+12 has been targeted in particular, both within surveys and by other specific observations. A range of wavelengths have been considered from visible (Abazajian et al. 2005) to near-IR (Cutri et al. 2003), mid-IR (Foster & Fischer 1996), far-IR (Moshir & et al. 1990), and sub-mm (Phillips & Chandler 1994; Greaves & Holland 2000; Löhmer et al. 2004). (A summary of these PSR B1257+12 observations is shown in Figure 1 below.) In each case, only upper limits for dust emission were obtained.

Nevertheless, these searches have been limited by their sensitivity, particularly at far-IR wavelengths. Very high upper limits for the dust mass ( $\sim 100 M_{\oplus}$ ) are commonly cited (Löhmer et al. 2004; Lazio & Fischer 2004). Pulsars tend to be much farther away than the main-sequence stars identified as having debris disks (typically tens of pc for solar-type

stars; Bryden et al. 2006), making detection more difficult. Perhaps more importantly, the pulsar’s efficiency in heating any dust that might be present may be much lower than for hydrogen-burning stars whose radiation peaks in visible light (see §3 below). Given the difficulty in detecting dust around pulsars, the *Spitzer Space Telescope*, with unprecedented sensitivity to infrared radiation, is an ideal observatory for continuing the ongoing search for dust in the PSR B1257+12 system. Below, we describe such *Spitzer* observations (§2) and then use them to place stricter limits on the PSR B1257+12 dust luminosity (§3).

## 2. Observations

PSR B1257+12 was observed with the *Spitzer* long-wavelength camera, MIPS, on 21 Jun 2005 at both 24 and 70  $\mu\text{m}$ . Our overall data analysis is similar to that previously described by Beichman et al. (2005b), Bryden et al. (2006), and Gautier et al. (2006). At 24  $\mu\text{m}$ , mosaiced images were created from the raw data using the DAT software developed by the MIPS instrument team (Gordon et al. 2005). Several additional corrections were applied, including the subtraction of smooth gradients across the field (to remove scattered light effects parallel to the scan mirror direction) and the application of a second-order flat, derived from the data itself (to correct for dark latents, residual jail-bars, and broad flat-field trends). At 70  $\mu\text{m}$ , images were processed beyond the standard DAT software to correct for time-dependent transients, corrections which can greatly improve the sensitivity of the measurements (Gordon et al. 2005). For both wavelengths, aperture photometry was performed using calibration factors, apertures sizes, background annuli, and aperture corrections as in Beichman et al. (2005b). PSR B1257+12 was not observed at 160  $\mu\text{m}$ , due to the high background noise in MIPS images at that wavelength (typically tens of mJy) relative to existing sub-mm limits.

At the observed wavelengths, we fail to detect significant emission from the pulsar system. Upper limits are calculated directly from the noise levels measured within each field. At 24  $\mu\text{m}$ , where we have integrated over 5 cycles of 3 sec exposures, we achieve a ( $1-\sigma$ ) sensitivity of 0.045 mJy. At 70  $\mu\text{m}$ , with 5 cycles of 10 sec exposures, our sensitivity is 1.45 mJy. This level of accuracy at 70  $\mu\text{m}$  is better than that typically seen in similar observations (e.g. Beichman et al. 2005b), a reflection of the fortuitously low background level in this field. The accuracy of this observation is likely to be limited by confusion with background extragalactic sources, such that longer integration time would not significantly improve the results (Dole et al. 2004; Bryden et al. 2006).

The  $3-\sigma$  upper limits calculated here are shown in Figure 1 alongside those from previous investigations. While  $\sim$ mJy limits have been obtained at near-IR and sub-mm wavelengths,

previous observations have been least sensitive at the far-IR wavelengths most commonly used to detect dust emission around main-sequence stars. At  $24\ \mu\text{m}$ , the *Spitzer* limit is more than three orders of magnitude better than IRAS, while at  $70\ \mu\text{m}$  there is a factor of  $\sim 40$  improvement. The following section translates these limits on flux into constraints on the dust temperature and luminosity.

### 3. Dust Constraints

Other searches for dust around PSR B1257+12 have generally compared their observational limits with the dust model of Foster & Fischer (1996). In this model, the dust absorbs and re-radiates some fraction of the energy that the pulsar is known to be losing as it spins down. This spin-down luminosity,  $L_{\text{SD}} = 4\pi^2 I \dot{P} / P^3$ , can be easily calculated from the pulsar’s period,  $P$ , and spin-down rate,  $\dot{P}$ . The pulsar’s moment of inertia,  $I$ , is assumed to be  $10^{45}\ \text{g cm}^2$  (Foster & Fischer 1996). For PSR B1257+12 ( $P = 6.2\ \text{ms}$ ,  $\dot{P} = 1.1 \times 10^{-16}\ \text{ms/s}$ ; Konacki & Wolszczan 2003) the spin-down luminosity is  $5.2\ L_{\odot}$ . Following Foster & Fischer (1996), previous work (e.g. Greaves & Holland 2000; Löhmer et al. 2004) typically assumed a dust luminosity of 1% of  $L_{\text{SD}}$ , a plausible upper limit for the fraction of energy a thick dust disk might intercept.

Rather than assume an ad hoc dust luminosity, we instead choose to treat  $L_{\text{dust}}/L_{\text{SD}}$  as the primary unknown quantity whose value we can place limits on. In fact, the dust luminosity can be directly constrained from flux measurements, depending on the temperature of the dust (e.g. Beichman et al. 2005b). The temperature, however, is very uncertain. The standard Foster & Fischer (1996) dust models assign temperatures of 10-20 K to the dust, but the physical mechanism for converting the pulsar’s rotational energy into thermal dust emission is not specified. The dust temperature in these models is essentially arbitrary. The ability of the various-sized dust grains to absorb the pulsar’s emitted energy is not considered, nor is the distance of the dust from that energy source.

Around solar-type stars, which emit radiation at wavelengths readily absorbed by micron-sized dust grains, dust at 1 AU can reach temperatures of several hundred K. Around pulsars with solar-like luminosities spread over a range of wavelengths, the absorption is presumably less efficient, resulting in lower temperatures at the same orbital distances. Should a belt of material circle outside the orbits of the PSR B1257+12 planets, temperatures of  $\sim 50$ -100 K might be expected, depending on the pulsar’s spectral distribution. The fraction of PSR B1257+12’s luminosity emitted at various wavelengths is directly limited by observations. Although the pulsar emission model of Malov (2003) predicts a high X-ray flux ( $5 \times 10^{-9}\ \text{erg cm}^{-2}\ \text{s}^{-1}$ ), the lack of detection by Chandra sets an upper limit of  $6 \times 10^{-15}\ \text{erg cm}^{-2}$

$\text{s}^{-1}$  (Pavlov et al. 2006), less than  $10^{-6}$  of the spin-down luminosity. Optical non-detections (e.g. Abazajian et al. 2005) provide similarly strict limits for visible emission. Instead, most of the pulsar’s spin-down energy is emitted as relativistic particles (Gaensler & Slane 2006). In this case, the heating of small dust grains is minimal; each particle impact with a dust particle will eject a nuclide from the system without imparting kinetic energy into the parent dust grain. The heating efficiency for the dust in a thin disk may then be very low, with correspondingly low temperatures. Rocks that are larger than the stopping depth for the relativistic particles ( $\sim 100$  cm; Miller & Hamilton 2001), however, will absorb most of the incoming energy and will be much more efficient at converting the pulsar’s spin-down energy into thermal radiation.

Unlike the highly beamed radio emission, pulsars’ particle winds are fairly symmetric, as evidenced by the near-spherical shapes of pulsar wind nebulae (e.g. Kennel & Coroniti 1984; Gaensler & Slane 2006). A key uncertainty, however, is the location where the pulsar’s magnetic dipole radiation transitions into a relativistic particle wind. Close to the pulsar, at its light cylinder radius ( $c/\Omega = 300$  km), the outward flow is thought to be dominated by the Poynting flux ( $E \times B$ ) (Gaensler & Slane 2006). Observations of pulsar nebulae, however, find that the flux on larger scales is concentrated in a particle wind. For the Crab Pulsar’s nebula, for example, modeling of the energy deposition into the wind termination shock requires that a large fraction ( $\gtrsim 99\%$ ) of the energy have been converted into a particle wind before reaching a few pc from the pulsar (Kennel & Coroniti 1984; Begelman & Li 1992). Exactly where or how transition occurs is not known. Assuming that the particle wind has fully developed before reaching  $\sim 1$  AU orbital distances, the pulsar’s spin-down energy will effectively heat all large bodies in the planetary system; otherwise only ionized matter would be strongly influenced.

Given the uncertainty in the dust temperature, we leave it as a free parameter to be constrained by observations. Figure 2 shows our constraints on  $L_{\text{dust}}/L_{\text{SD}}$  for a range of dust temperatures, under the assumption that the dust can be characterized by a single dominant value. (In reality some range of temperatures would exist for dust with a range of grain sizes and orbital locations, even more so if stochastic heating is responsible for large temporary increases in dust temperature for a small fraction of the grains.) For each temperature, we calculate the maximum blackbody emission that is consistent with the observed  $3\text{-}\sigma$  limits. Each of the curved segments in Figure 2 corresponds to an individual observation at a specific wavelength, with the temperatures that an observation is most sensitive to depending on that wavelength. As seen in the figure, the *Spitzer* observations create more stringent limits on dust luminosity for dust with temperatures between 20 and 1000 K. (Above 1000 K, near-IR photometry is more accurate, while below 20 K sub-mm measurements are more sensitive.) Better than two orders of magnitude improvement in sensitivity is achieved over much of

this range, with limits on  $L_{\text{dust}}$  as low as  $2.5 \times 10^{-5} L_{\text{SD}}$  for  $\sim 150$  K dust. For high-emissivity dust orbiting at 2.5 AU, this corresponds to an upper limit on the emitting area of  $5 \times 10^{23}$  cm<sup>2</sup>.

#### 4. Discussion

Based on our *Spitzer* observations, we constrain the luminosity of dust emission around PSR B1257+12 to be  $< 10^{-4} L_{\text{SD}}$  for temperatures of  $\sim 50$  to 500 K. This limit allows us rule out a dense, thick disk that absorbs and thermalizes a large fraction of the emitted energy - essentially the same general conclusion as reached by previous authors. This non-detection of IR excess, however, does not exclude the presence of an optically thin debris disk orbiting the pulsar. While the *Spitzer* observations represent a great improvement over previous IR observations, they still do not have an optimal level of accuracy in terms of  $L_{\text{dust}}/L_{\text{SD}}$ . Observations of nearby main sequence stars at this sensitivity level would be able to detect only the brightest debris disks. For example, only  $\sim 2\%$  of solar-like type stars have luminosities  $> 10^{-4} L_{\star}$  (Bryden et al. 2006). A much greater fraction of these stars ( $\sim 12\%$ ) have disks within an order of magnitude below this limit, while the Solar System has  $L_{\text{dust}}/L_{\star}$  even lower ( $\sim 10^{-7}$  to  $10^{-6}$  for the Kuiper Belt; Stern 1996). Even if the dust is efficiently heated by the pulsar, there may simply be too little for us to detect.

A belt of planetesimals circling at a few AU, similar to our own asteroid belt, might still be expected. In other systems, the detection of emitting dust outside of the orbits of known extrasolar planets (Beichman et al. 2005b), similar to the Kuiper Belt in our Solar System, suggests that an architecture of outer debris belts encircling inner planets may be a general consequence of planet formation. Goździewski et al. (2005), meanwhile, have investigated the long-term stability of test particles orbiting in the PSR B1257+12 system, finding that most of the region outside of 1 AU is stable to perturbations from the three inner planets. While high energy particles emitted from the pulsar should evaporate very small bodies on a relatively short time scale, Miller & Hamilton (2001) estimate that planetesimals larger than  $\sim$ km in size can survive the lifetime of the pulsar. (The age of the pulsar is estimated from its spin-down time scale,  $P/2\dot{P}$ , to be  $< \text{Gyr}$ .) In fact, there is now evidence for an asteroid-like object orbiting at 2.4 AU with a mass of  $4 \times 10^{-4} M_{\oplus}$ , about twice the mass of Ceres, the largest asteroid in the Solar System (Wolszczan & Konacki 2006). Ongoing pulsar timing measurements will probe down to even smaller masses and can eventually determine whether many large asteroids are present in this system.

From this pulsar timing, some bounds can be placed on the total mass contained in larger planetesimals. Pulsar timing measurements provide direct constraints on the mass

distribution, which is restricted to large asteroid-like mass concentrations. For an extended disk, the total mass potentially contained in asteroids is limited by the requirement that the belt not grind itself away over lifetime of the system. If the age of the pulsar is  $\sim$ Gyr, the time scale for destructive collisions between the largest objects must be longer in order for them to survive. A disk with tens of Earth masses of planetesimals would break itself down into smaller objects relatively quickly. The Solar System’s asteroid belt, by comparison, is evolving on gigayear time scales (Dermott et al. 2002). Similarly, the collisional time scale for a disk of planetesimals a few AU from a pulsar is of order  $\sim R_{\text{pl}}M_{\oplus}/R_{\oplus}M_{\text{disk}}$  Gyr, where  $R_{\text{pl}}$  is the typical size of the planetesimals and  $M_{\text{disk}}$  is their combined mass (see e.g. Dominik & Decin 2003), such that a  $1\text{-}M_{\oplus}$  disk of planetesimals would have ground down already.

The mass contained in smaller bodies is less clear. Given the possibility of weak coupling between dust and the energy emitted by the pulsar, the observational constraints on dust luminosity do not translate well into upper limits on dust mass in the system. Rapid dust removal, however, suggests that the dust mass not be arbitrarily large. If the disk is optically thin toward the pulsar wind, dust particles will be ablated by relativistic particle impacts on time scales of  $< 1$  yr (Miller & Hamilton 2001), i.e. even faster than the removal of Solar System dust by Poynting-Robertson drag ( $\sim 10^3$  yr for  $\mu\text{m}$ -sized grains; Gustafson 1994). As in our own system, dust could be continually replenished by a collisional cascade from larger rocks, but the fast removal process would limit the amount of dust to a level below that from a similar cascade around a main-sequence star.

In order to assess the effect of this ablation on the infrared emission from a pulsar encircling debris disk, we consider a collisional cascade model in which large planetesimals are continuously shattered to produce smaller and smaller objects. The equilibrium slope of the resultant distribution is  $dn/da \propto a^{-3.5}$  (Dohnanyi 1968), such that the smallest grains dominate the overall surface area while the largest bodies comprise the bulk of the system’s mass. On top of this standard collisional cascade we have included the important new effect in a pulsar environment - particle ablation by the pulsar wind. Otherwise the simulations we present here are relatively simple compared to detailed asteroid belt models (e.g. Durda & Dermott 1997). In particular, we assume that 1) the binding strength is independent of object size, 2) impactors can catastrophically disrupt objects up to ten times their size, and 3) the distribution of debris created in such an impact goes as  $dn/da \propto a^{-3.5}$ . While these simplifications neglect some of the physics (for a full discussion and detailed models see Davis et al. (2002)), they allow us to calculate illustrative models of the dust surrounding a pulsar.

Before including the effects of the pulsar wind, we start with a standard collisional cascade similar to our own asteroid belt’s. Starting with  $10 M_{\oplus}$  of 500 km radius planetesimals

located at 2.5 AU, after 1 Gyr of collisions the belt of material has ground down to just  $10^{-2}M_{\oplus}$  (c.f.  $\sim 10^{-3}M_{\oplus}$  contained in the asteroid belt; Davis et al. 2002). The resultant size distribution (*dashed line* in Figure 3) extends from the large planetesimals down to small dust. For grain sizes smaller than  $\sim$ mm, Poynting-Robertson drag begins to remove dust faster than it can be replenished by collisions, resulting in a small but significant flattening of the size distribution for the smallest grains. In the Solar System, for example, the combination of collisions and P-R drag result in a typical dust radius of several 100  $\mu$ m within the asteroid belt (Dermott et al. 2002) while the interstellar dust particles reaching the Earth have sizes somewhat smaller ( $\sim 100 \mu$ m; Love & Brownlee 1993). The total dust area in our collisional model without ablation is  $5 \times 10^{22} \text{ cm}^2$ . For a given total mass, varying the unknown material composition tends to have relatively little effect on this dust area (denser material has less emitting area per mass, but is more resistant to removal by radiation pressure; in the simple model considered here these effects exactly offset each other).

At the other extreme we also consider the distribution of object sizes under the influence of ablation, but with no collisions (*dotted line* in Figure 3). This would apply to a very sparse distribution of planetesimals. As calculated by Miller & Hamilton (2001), objects up to several km in size are worn down by the pulsar wind over 1 Gyr. The other important size scale for this distribution is 100 cm, the stopping distance for the relativistic particles. For objects larger than this, mass loss is independent of size (giving equal numbers of objects in linear mass bins or  $dn/d(\log a) \propto a^3$ ) while below 100 cm the mass loss is directly proportional to mass (giving equal numbers in logarithmic mass bins or  $dn/d(\log a) = \text{constant}$ ).

When collisions are again considered in addition to the effects of ablation (*solid line* in Figure 3), objects smaller than km in size are continually resupplied by the disruptive collisions of larger objects. This replenishment greatly increases the amount of small dust and rocks above the simple ablation estimate (compare the *dotted* and *solid* lines in Figure 3). The ability of Poynting-Robertson drag to remove the smallest dust is unclear. (P-R drag is caused by particles absorbing photons with no angular momentum and then re-emitting them in the dust’s rotating frame. The particles emitted by the pulsar as it spins down, however, do carry their own positive angular momentum which they would then impart on the dust grains.) Regardless of whether or not many sub-micron grains are present, their heating by the pulsar wind is very inefficient, as mentioned above. The larger planetesimals, on the other hand, are thick enough to absorb the pulsar’s emission energy, and should reach temperatures comparable to the local blackbody temperature (270 K at 2.5 AU). As in the pure ablation case, the majority of the warm surface area in the system continues to be contributed by these large  $\sim$ km-sized objects. The total emitting cross section for the model distribution is  $4 \times 10^{19} \text{ cm}^2$ . This is a factor of 5 greater than with ablation alone (*dotted line*), but still three orders of magnitude less than the area around the standard collisional



cascade without ablation (*dashed line*). This area at 2.5 AU corresponds to  $L_{\text{dust}}/L_{\text{SD}}$  of just  $2.3 \times 10^{-9}$ , far below our observational limit.

Models in which disks steadily and smoothly grind away with time, however, fail to describe the variety of debris disks now observed with *Spitzer*. Just considering analytic models like those in Figure 3, one might conclude that all systems would grind down their asteroid belts in a similar fashion to our own, such that no old stars should have observable inner belts. This is in contrast with systems such as HD 69830, which has a bright disk of small dust grains orbiting at  $\sim 0.5$  AU ( $L_{\text{dust}}/L_{\star} \sim 2 \times 10^{-4}$ ; Beichman et al. 2005a). Despite the old age of this star ( $\sim 2$  Gyr), the debris has an emitting surface area more than 1000 times greater than our asteroid belt’s. As is clear from the collisional models, such a situation cannot persist for the lifetime of the star, but instead must be a reflection of some recent spike in activity. Based on the broad halo of small, short-lived dust grains blown out from Vega’s debris disk, a large recent collisional event is also inferred in that system (Su et al. 2005). More generally, Rieke et al. (2005) find that while debris disk frequency declines as stars age, even old A stars can have significant emission due to stochastic collisional events, while Bryden et al. (2006) similarly find many bright disks among even older FGK stars. Overall, one can conclude that many, if not most, observed debris disks are observable only because an unusual event has recently increased their infrared brightness. Such collisional events will also cause temporary enhancements of the infrared emission from debris disks around pulsars. Although the model in Figure 3 is four orders of magnitude below the observational threshold presented in §3, modest improvements in the detection limit could detect the aftereffects of a large collisional event like those commonly seen around main sequence stars, if one has recently occurred in the PSR B1257+12 system.

We conclude that, despite our new limits on IR excess, a  $0.01 M_{\oplus}$  belt of 100-km-sized asteroids and its collisionally produced dusty debris may still be present in this system. Whether or not this debris could be detected at far-infrared wavelengths depends strongly on its recent collisional history.

This publication makes use of NASA/IPAC’s InfraRed Science Archive (IRSA) which provides access to data from the 2MASS and IRAS all-sky surveys. The *Spitzer Space Telescope* is operated by the Jet Propulsion Laboratory, California Institute of Technology, under NASA contract 1407. Development of MIPS was funded by NASA through the Jet Propulsion Laboratory, subcontract 960785. Some of the research described in this publication was carried out at the Jet Propulsion Laboratory, California Institute of Technology, under a contract with the National Aeronautics and Space Administration. We would like to thank Tom Kuiper for discussions on pulsar emission and an anonymous referee for helpful comments.

## REFERENCES

- Abazajian, K., Adelman-McCarthy, J. K., Agüeros, M. A., et al. 2005, *AJ*, 129, 1755
- Aumann, H. H., Beichman, C. A., Gillett, F. C., et al. 1984, *ApJ*, 278, L23
- Beckwith, S. V. W., Sargent, A. I., Chini, R. S., & Guesten, R. 1990, *AJ*, 99, 924
- Begelman, M. C. & Li, Z.-Y. 1992, *ApJ*, 397, 187
- Beichman, C. A., Bryden, G., Gautier, T. N., et al. 2005a, *ApJ*, 626, 1061
- Beichman, C. A., Bryden, G., Rieke, G. H., et al. 2005b, *ApJ*, 622, 1160
- Bryden et al., G. 2006, *ApJ*, 636, 1098
- Cordes, J. M. & Lazio, T. J. W. 2002
- Cutri, R. M., Skrutskie, M. F., van Dyk, S., et al. 2003, *VizieR Online Data Catalog*, 2246
- Davis, D. R., Durda, D. D., Marzari, F., Campo Bagatin, A., & Gil-Hutton, R. 2002, *Asteroids III*, 545
- Dermott, S. F., Durda, D. D., Grogan, K., & Kehoe, T. J. J. 2002, *Asteroids III*, 423
- Dohnanyi, J. S. 1968, in *IAU Symp. 33: Physics and Dynamics of Meteors*, 486
- Dole, H., Rieke, G. H., Lagache, G., et al. 2004, *ApJS*, 154, 93
- Dominik, C. & Decin, G. 2003, *ApJ*, 598, 626
- Durda, D. D. & Dermott, S. F. 1997, *Icarus*, 130, 140
- Foster, R. S. & Fischer, J. 1996, *ApJ*, 460, 902
- Gautier et al., T. N. 2006, *ApJ*, in preparation
- Gaensler, B. M. & Slane, P. O. 2006, *ARA&A*, 44, 1
- Gordon, K. D., Rieke, G. H., Engelbracht, C. W., et al. 2005, *PASP*, 117, 503
- Gordon et al., K. D. 2005, *SPIE*, 5487, in press
- Goździewski, K., Konacki, M., & Wolszczan, A. 2005, *ApJ*, 619, 1084
- Greaves, J. S. & Holland, W. S. 2000, *MNRAS*, 316, L21

- Gustafson, B. A. S. 1994, *Annual Review of Earth and Planetary Sciences*, 22, 553
- Habing, H. J., Dominik, C., Jourdain de Muizon, M., et al. 2001, *A&A*, 365, 545
- Kennel, C. F. & Coroniti, F. V. 1984, *ApJ*, 283, 710
- Koch-Miramond, L., Haas, M., Pantin, E., et al. 2002, *A&A*, 387, 233
- Konacki, M. & Wolszczan, A. 2003, *ApJ*, 591, L147
- Löhmer, O., Wolszczan, A., & Wielebinski, R. 2004, *A&A*, 425, 763
- Lazio, T. J. W. & Fischer, J. 2004, *AJ*, 128, 842
- Lin, D. N. C., Woosley, S. E., & Bodenheimer, P. H. 1991, *Nature*, 353, 827
- Love, S. G. & Brownlee, D. E. 1993, *Science*, 262, 550
- Malov, I. F. 2003, *Astronomy Letters*, 29, 502
- Marcy, G. W. & Butler, R. P. 1995, *Bulletin of the American Astronomical Society*, 27, 1379
- Mayor, M. & Queloz, D. 1995, *Nature*, 378, 355
- McCaughrean, M. J. & O'Dell, C. R. 1996, *AJ*, 111, 1977
- Michel, F. C. & Dessler, A. J. 1985, *Science*, 228, 1015
- Miller, M. C. & Hamilton, D. P. 2001, *ApJ*, 550, 863
- Moshir, M. & et al. 1990, in *IRAS Faint Source Catalogue*, version 2.0, 1
- Pavlov et al. 2006, *ApJ*, in preparation
- Phillips, J. A. & Chandler, C. J. 1994, *ApJ*, 420, L83
- Podsiadlowski, P., Pringle, J. E., & Rees, M. J. 1991, *Nature*, 352, 783
- Rieke, G. H., Su, K. Y. L., Stansberry, J. A., et al. 2005, *ApJ*, 620, 1010
- Stern, S. A. 1996, *A&A*, 310, 999
- Stevens, I. R., Rees, M. J., & Podsiadlowski, P. 1992, *MNRAS*, 254, 19P
- Su et al., K. 2005, *ApJ*, submitted
- Tavani, M. & Brookshaw, L. 1992, *Nature*, 356, 320

Taylor, J. H. & Cordes, J. M. 1993, ApJ, 411, 674

van Buren, D. & Terebey, S. 1993, in ASP Conf. Ser. 36: Planets Around Pulsars, 327–333

Wolszczan, A. 1994, Science, 264, 538

Wolszczan, A. & Frail, D. A. 1992, Nature, 355, 145

Wolszczan, A., Hoffman, I. M., Konacki, M., Anderson, S. B., & Xilouris, K. M. 2000, ApJ, 540, L41

Wolszczan, A. & Konacki, M. 2006

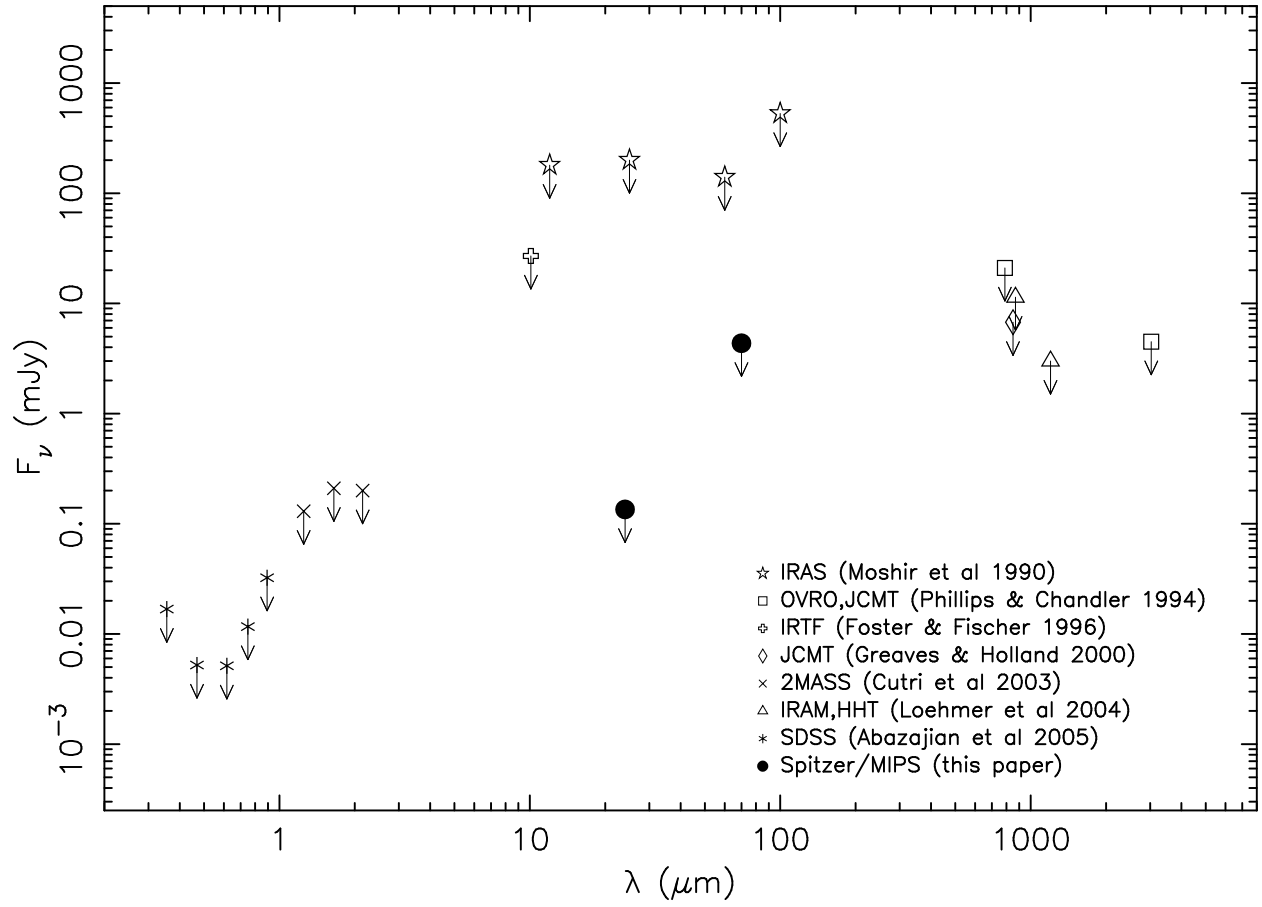


Fig. 1.— Observational upper limits for emission from the PSR B1257+12 system. Over a range of wavelengths from visible to mm,  $3\text{-}\sigma$  upper limits are shown for data from various sources (see legend). Our MIPS 24 and 70  $\mu\text{m}$  results are shown as filled circles.

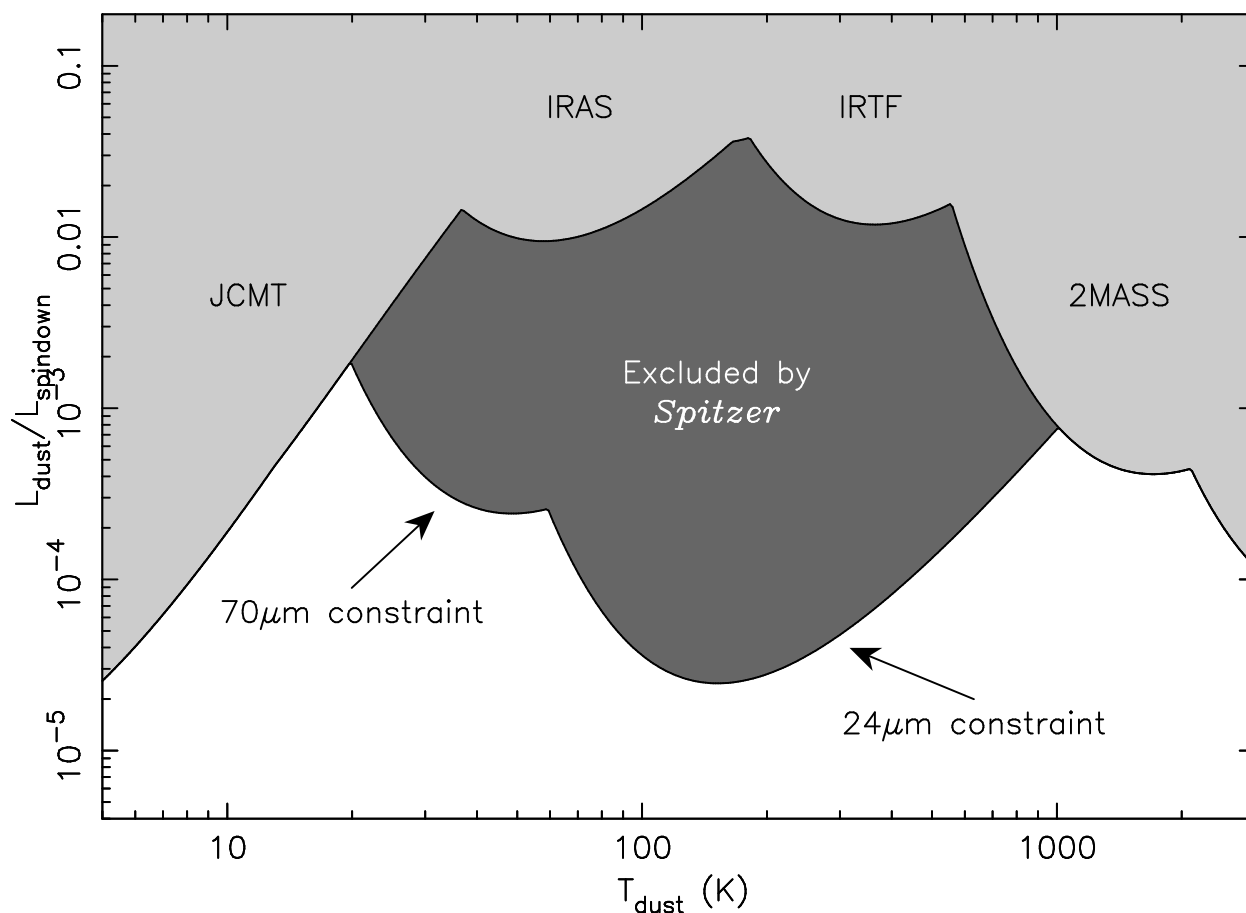


Fig. 2.— Limits on the temperature and luminosity of dust in the PSR B1257+12 system. The light shaded region is based on previous observations, while the dark shaded region represents dust parameters ruled out by the observations described here. Dust emissivity is assumed to fall off linearly as the wavelength increases past  $100 \mu\text{m}$ . To convert fluxes to luminosities, we adopt a pulsar distance of 450 pc based on the Taylor & Cordes (1993) model for the galactic electron distribution, recently updated by Cordes & Lazio (2002); this distance is uncertain by  $\sim 20\%$ .

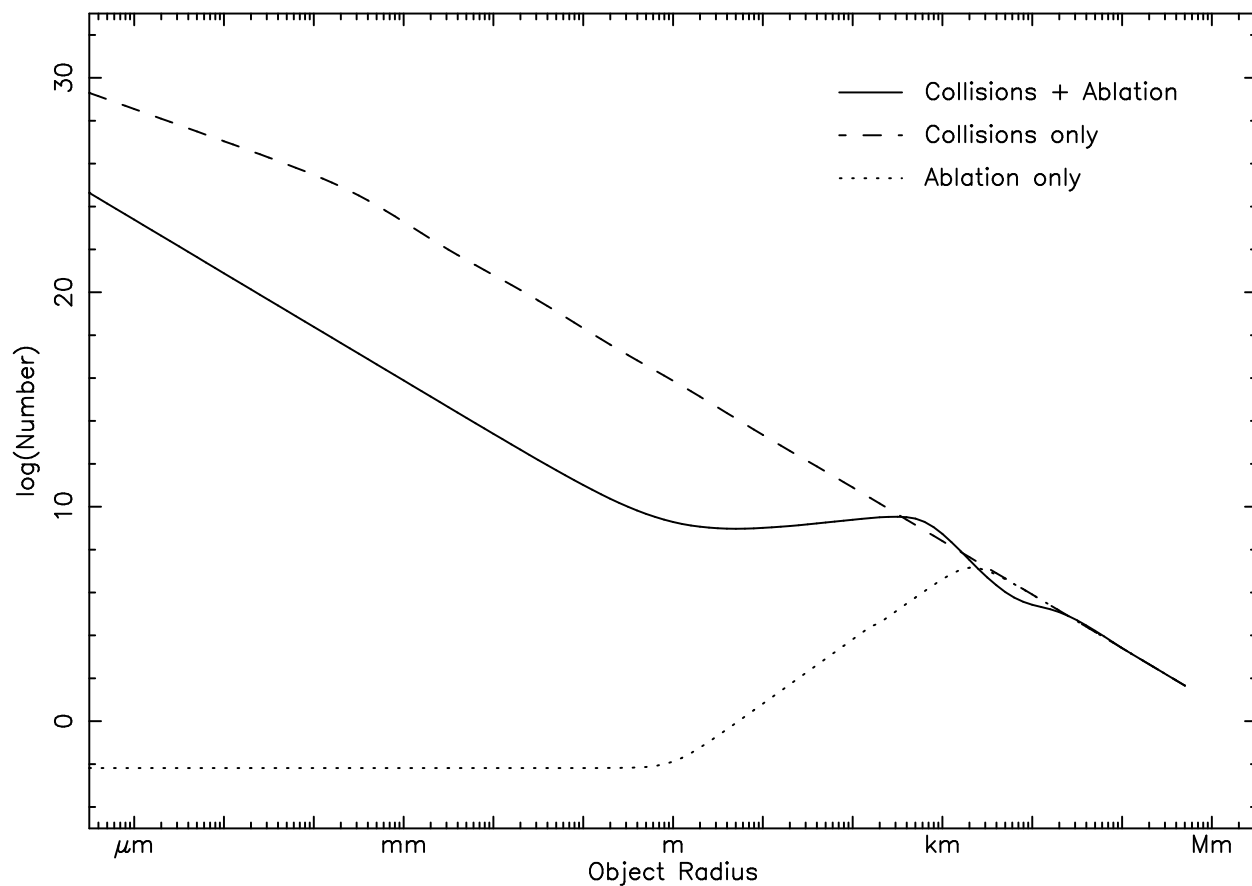


Fig. 3.— Distribution of particle sizes in a system with strong ablation by a relativistic particle wind. Sizes ranging from  $\mu\text{m}$ -sized dust up to 500 km radius planetesimals are considered. The number of particles is given per logarithmic size bin. Below  $\sim 1$  km in radius, objects are ablated by the pulsar wind faster than they are replenished by collisions of larger sized objects. The distribution of particle sizes produced by a standard collisional cascade is shown for comparison (dashed line), as is the case with ablation but no collisions (dotted line).